



Published in final edited form as:

*Stem Cell Rev.* 2013 October ; 9(5): 655–667. doi:10.1007/s12015-013-9442-7.

## SCF promotes dental pulp progenitor migration, neovascularization, and collagen remodeling – potential applications as a homing factor in dental pulp regeneration

Shuang Pan<sup>1,2</sup>, Smit Dangaria<sup>2</sup>, Gokul Gopinathan<sup>2</sup>, Xiulin Yan<sup>2</sup>, Xuanyu Lu<sup>2</sup>, Antonia Kolokythas<sup>3</sup>, Yumei Niu<sup>1</sup>, and Xianghong Luan<sup>2,\*</sup>

<sup>1</sup> Harbin Medical University, School of Dentistry, Department of Endodontics

<sup>2</sup> UIC College of Dentistry, Department of Oral Biology

<sup>3</sup> UIC College of Dentistry, Department of Oral Surgery

### Abstract

Stem cell factor (SCF) is a powerful chemokine that binds to the c-Kit receptor CD117 and has shown promise as a homing agent capable of progenitor cell recruitment. In the present study we have documented high levels of both SCF and its receptor c-Kit in differentiating dental pulp (DP) cells and in the sub-odontoblastic layer of Höhl. *In vitro* studies using human DP progenitors revealed a significant increase in cell proliferation after 100nM SCF application, explained by a 2-fold upregulation in cyclin D3 and FGF2 cell cycle regulators, and a 7-fold increase in CDK4 expression. DP cell migration in the presence of SCF was up-regulated 2.7-fold after a 24 hour culture period, and this effect was accompanied by cytoskeletal rearrangement, a 1.5-fold increase in polymeric F-actin over G-actin, and a 1.8-fold increase in RhoA expression. Explaining the signaling effect of SCF on DP migration, PI3K/Akt and MEK/ERK pathway inhibitors were demonstrated to significantly reduce DP cell migration, while SCF alone doubled the number of migrated cells. ERK and AKT phosphorylation were dramatically upregulated already 3-5 minutes after SCF addition to the culture medium and declined thereafter, classifying SCF as a fast acting chemokine. When applied as an agent to promote tissue regeneration in subcutaneously implanted collagen sponges, SCF resulted in a 7-fold increase in the cell number in the implanted tissue construct, a more than 9-fold increase in capillaries, as well as collagen sponge remodeling and collagen fiber neogenesis. Together, these studies demonstrate the suitability of SCF as a potent aid in the regeneration of dental pulp and other mesenchymal tissues, capable of inducing cell homing, angiogenesis, and tissue remodeling.

### Introduction

Mesenchymal stem cells possess great capacity for tissue regeneration, either by directly replacing diseased and lost tissues through local implantation or by recruiting endogenous stem cells from the blood or from adjacent stem cell niches. Tissue regeneration through

\*Address for Correspondence Xianghong Luan, MD Associate Professor UIC Brodie Laboratory for Craniofacial Genetics 801 South Paulina Chicago, IL 60612 luan@uic.edu.

The authors declare no potential conflicts of interest.

local delivery of *ex vivo* cultured cells faces a number of experimental and clinical challenges, including limited availability of autologous stem cells, stem cell propagation outside of the human body, and the need for site-specific replantation of functional cell populations altered by factors and culture conditions. To overcome the limitations of *ex vivo* grown stem cell transplants, recent reports have explored the recruitment of endogenous progenitor cells as a novel strategy for *in situ* tissue regeneration [1-4]. This active navigation of stem cells toward target sites is called homing [5,6]. Homing involves trafficking of stem cells to sites of injury and subsequent participation in regeneration of lost or diseased tissue [6]. The most frequently studied homing model is the transplantation of hematopoietic stem cells, involving a series of steps, including (i) signaling by stromal-derived factor 1 (SDF-1) and stem cell factor (SCF), (ii) activation of lymphocyte function-associated antigen 1 (LFA-1) and CD44, (iii) cytoskeletal rearrangement, (iv) matrix metalloproteinase activation and secretion of MMP2/9, (v) rolling and firm adhesions of progenitors to endothelial cells, (vi) trans-endothelial migration across the extracellular matrix barrier, and (vii) selective migration and anchorage to specialized stem cell niches [5]. While especially well characterized in blood, homing as a strategy for tissue regeneration has also been successfully applied in other tissues such as musculoskeletal tissues [6], heart [7], and teeth [8].

Embedded between mineralized tissues, teeth feature two distinct soft tissues that have recently been the focus of cell homing studies, the dental pulp and the periodontal ligament [8-10]. Regeneration of dental pulp tissues is the ultimate goal of biological endodontics [11], while periodontal regeneration serves to provide new and healthy attachment for diseased teeth [12,13]. In previous studies, pulp tissues were regenerated using a pulp-slice model [14-16] or subcutaneous implants [11] to demonstrate the regenerative capability of dental pulp stem cells [17]. In contrast, recent cell homing studies exploited the chemotactic effects of SDF-1 to recruit dental pulp-like cells into collagen scaffolds or subcutaneously implanted tooth roots, or other cells into the periphery of anatomically shaped tooth scaffolds [9]. Most recently, complete pulp regeneration was accomplished after pulpectomy and transplantation of CD105<sup>+</sup> stem cells in combination with SDF-1 [18].

SDF-1 and SCF are two prominent homing factors that have recently emerged as aids in regenerative medicine. SDF-1 has been reported to recruit marrow-derived CD34 cells and other cells to the site of injury, and SCF and SDF-1 act synergistically to increase the chemotaxis of CD34 cells *in vitro*, suggesting that both play a role in the recruitment of stem cells [19,20]. Both homing factors, SDF-1 and SCF, are chemokines that have the ability to mobilize stem cells and attract them toward homing sites. They are reported to share signaling pathways in hematopoietic progenitors and to synergize [21]. SDF-1 functions as the ligand for the chemokine receptor 4 (CXCR4), while SCF dimerizes with the tyrosine kinase proto-oncogene Kit (c-Kit), resulting in phosphorylation and signal transduction related to proliferation and differentiation [22,23]. Similar to SDF-1, SCF enhances the mobilization and trafficking of progenitor cells [24,25]. In tissue engineering applications, SCF has been successfully used to promote cardiac repair [26], liver regeneration [20], neurogenesis [27], corneal wound healing [28], and germ cell maintenance [29], but not yet in craniofacial and dental applications.

In the present study, we have thus examined whether c-Kit and its ligand SCF are expressed in teeth and whether they may be useful as homing agents for the recruitment of progenitor cells. After mapping SCF and c-Kit expression to dental pulp cells and odontoblasts, the effect of SCF on dental pulp progenitors and on the recruitment of cells into tissue engineering constructs were examined. Based on the relationship between SCF/c-Kit and extracellular matrix components [30,31], we have then identified mechanisms by which SCF might affect the mobilization and homing of dental pulp progenitors. Together, the present study examines expression, extracellular matrix pathways, and tissue engineering potential of the chemokine SCF and its ligand c-Kit.

## Material and Methods

### Tissue processing

CD1 mice were obtained from Charles River (Wilmington, MA) and bred at UIC in strict accordance with the recommendations on the Guide for the Care and Use of Laboratory Animals of the National Institutes of Health. The protocol was approved by the Committee on the Ethics of Animal Experiments of the University of Illinois at Chicago. Mandibles from postnatal day 3 CD1 mice were dissected and fixed with 10% formalin at 4°C. For decalcified paraffin sections, mandibles were de-mineralized in EDTA, and processed for paraffin sections. Sections were subjected to immunohistochemistry.

### Isolation of human dental mesenchymal progenitors

Healthy human teeth (patients ranging from 12 to 15 years) extracted for orthodontic reasons in accordance with the human subjects protocol approved by the UIC's Institutional Review Boards and the Office for the Protection Research Subjects. Dental follicle (DF), dental pulp (DP), alveolar bone (AB) and periodontal ligament (PDL) were dissected from the developing tooth organs, and mesenchymal progenitors were isolated from the dental tissues after digestion with collagenase/dispase as described before [32].

### Immunohistochemistry and immunofluorescence

Sections were deparaffinized, rehydrated, and treated with 6% peroxide and methanol followed by a brief incubation in 10 mM sodium citrate buffer with 0.05% Tween 20 at pH 6.0 for antigen retrieval. After blocking, sections were first incubated with anti-SCF or anti-c-Kit antibody (Abcam, Cambridge, MA) at a dilution of 1:200, and then with anti-rabbit secondary antibody (Abcam) at a dilution of 1:2000. Protein expression was detected with a Histomouse Broad Spectrum AEC kit (Invitrogen, Carlsbad, CA) under a light microscope. As a negative control, non-immune rabbit serum was used instead of the primary antibody. For fluorescent immunohistochemistry, dental pulp mesenchymal progenitors (DP cells) were cultured on glass slides for 12 hours and fixed in 0.1% paraformaldehyde. The samples were incubated with rabbit anti-SCF or anti-c-Kit antibody overnight at 4 °C with a 1:200 dilution and then with secondary FITC-conjugated or Texas Red-conjugated anti-rabbit antibody (Invitrogen) for 10 min. Immunoreactivity was observed under fluorescence microscope.

### RNA extraction and RT PCR

Total RNAs were isolated from dental papilla or cultured cells using the TRIZOL LS Reagent (Invitrogen) according to the manufacturer's instructions. Two micrograms of total extracted RNA was applied toward cDNA generation with the Sprint RT Complete kit® (Clontech, Mountain View, CA). To quantify the mRNA expression levels of genes related to proliferation and extracellular matrix remodeling, real-time PCR primers were designed based on EMBL/GenBank searches (shown in Table I). Real-time PCR was performed using sequence specific sybergreen primers, and the ABI Prism 7000 Sequence detection system (Applied Biosystems, Foster City, CA). Reaction conditions were as follows: 2 min at 50 °C (one cycle), 10 min at 95 °C (one cycle), and 15 sec at 95 °C, and 1 min at 60 °C (40 cycles). Samples were normalized using  $\beta$ -actin or GAPDH. The analyses were performed in triplicate for three independent experiments to confirm reproducibility of the results. Relative expression levels were calculated using the  $2^{-Ct}$  method [33], and values were graphed as the mean expression level  $\pm$  standard deviation. Some PCR products were separated by electrophoresis in 2% agarose gels, stained with ethidium bromidine and visualized under UV light.

### Protein extraction and western blot analysis

For protein extraction, cultured DP cells were collected and subjected to various forms of treatment described elsewhere in the paper. Equal amounts of protein extracts in a lysis buffer containing 100mM Tris HCl pH 9.0, 200 mM KCl, 25 mM EGTA, 36 mM MgCl<sub>2</sub>, 2% deoxycholic acid and 10% DTT v/v were subjected to SDS–polyacrylamide gel electrophoresis, and the separated proteins were transferred to a PVDF membrane (Immobilon P®, Millipore, Billerica, MA). The membrane was incubated with anti-SCF, c-Kit, RhoA, pho-AKT, pan AKT, pho-ERK, ERK, or GAPDH primary antibodies (Abcam). Immune complexes were detected with peroxidase-conjugated secondary antibody (Molecular Probes®, Carlsbad, CA) and enhanced by chemiluminescence reagents (Pierce Biotechnology, Rockford, IL). The amounts of protein expression were compared after normalization against GAPDH as an internal calibrator in each lane.

### Alkaline phosphatase activity assay and Alizarin Red staining

After 7 days of culture in osteogenic media, cells were washed and stained with alkaline phosphatase substrate (Roche Diagnostic, Indianapolis, IN) to verify early osteogenic activity. After 21 days of culture in osteogenic media, cells were fixed with methanol, stained with 10% alizarin red solution, and mineralized nodules were identified as red spots on the culture dish.

### MTT cell proliferation assay

DP cells were cultured in 96-well plates for a defined time period (1-7 days). Prior to termination of culture, cells were incubated in MTT solution (2mg/ml of MTT in DMEM with 2% FBS) for 4 hours. To quantify proliferative activity, the MTT stained cells were lysed in HCL/Isopropanol, and the absorbance was detected at 570nm with background subtraction at 630nm.

### Cell migration assay

Cell migration assays were performed using the FluoroBlock-24-multiwell insert system (DB Biosciences, Bedford, MA). A series of concentrations of SCF were added into the culture medium in the lower chambers. Serum starved cells ( $10^5$ ) were seeded into each insert and allowed to migrate to the underside of the membrane for 24 hours. The non-migrated cells on the upper surface of the membrane were removed with a cotton swab, and the migratory cells attached to the lower surface were stained with DAPI. The number of migrated cells per membrane was counted using a Leica DMRX fluorescent microscope.

### Rhodamine phalloidin F-actin staining

The cultured cells were fixed with 3.7 % formalin, permeabilized with 0.1 % Triton-100, and then stained with rhodamine -conjugated phalloidin (Sigma). Phalloidin stabilized microfilaments were captured under a Leica DMRX fluorescent microscope.

### G-actin/F-actin ratio measurement

The ratio of G-actin and F-actin in DP cells was investigated using a G-actin/F-actin *in vivo* assay kit (Cytoskeleton Inc, Denver, CO) according to the manufacturer's instructions. Briefly, DP cells were homogenized in cell lysis and F-actin stabilization buffer. The cell lysate was centrifuged for 1 hour at 100,000g to separate polymer filamentous F-actin from monomer soluble G-actin. The pellets were then re-suspended. Equal amounts of both supernatant (G-actin) and the resuspended pellet (F-actin) were subjected to Western blot analysis using anti-actin antibody (Cytoskeleton). The ratio of G-actin and F-actin was calculated using densitometry.

### In vivo subcutaneous implantation experiments

20  $\mu$ l of SCF aqueous solution (50 ng/ml) was dropped on a collagen sponge sheet ( $3 \times 3 \times 3$  mm<sup>2</sup>) and incubate at room temperature for 1 hour to coat the scaffold surface. 20  $\mu$ l of PBS was used as a control. The swollen collagen sponges were mixed with the suspension of human DP progenitors at a density of  $10^6$  cells/50  $\mu$ l, followed by incubation for 3 hours at 37 °C for the collagen sponge incorporating DP cells. Four groups of collagen sponge constructs (control, SCF alone, DP cells alone and SCF plus DP cells) were implanted into the back of nude mice (male, 6 weeks of age, Charles River) below the subcutis, either directly or after incubation in the tooth pulp chamber. The experiments were terminated 4 weeks after implantation, and the implants were dissected and prepared for histological examination.

### Collagen fiber staining

De-paraffinized and re-hydrated collagen implants were stained in methyl blue solution for 5 minutes and examined using a light microscope.

### Statistical analysis

Quantitative data were presented as means  $\pm$  SD from three independent experiments and compared with one way ANOVA statistical analysis tests. The difference between groups was considered statistically significant at  $P < 0.05$ .

## Results

### **SCF was expressed in differentiating dental pulp, odontoblasts, and ameloblasts, while c-Kit was homogeneously distributed throughout the dental pulp of molar tooth organs**

To visualize the localization of the SCF and c-Kit proteins in developing tooth organs, sections from mandibles of PN3 mice were subjected to immunohistochemical analysis. SCF protein was strongly localized in the ameloblasts, differentiating odontoblasts, and adjacent subodontoblastic dental pulp cells of the first molar (Figs. 1A and 1C). The expression of c-Kit was absent in the ameloblasts and less intense in the odontoblasts and dental pulp cells of the second molar, which was at an earlier stage of morphogenesis (Figs. 1B and 1D). In contrast to the specific location of SCF expression, c-Kit protein was homogeneously distributed in the dental pulp tissue of the first molar (Figs. 1C and 1D) and at low levels in the second molar (Figs. 1E and 1F). The unique expression pattern of SCF in odontoblasts and dental pulp cells indicates that SCF may play a role in dentinogenesis. To understand the function of SCF/c-Kit in tooth morphogenesis, dental papilla tissues were dissected from developing tooth organs at postnatal days 1, 3, 5 and 7. RT-PCR analysis revealed that both SCF and c-Kit mRNAs were expressed in tooth molars, and the expression levels increased during development (Fig. 1I). To explore the presence of SCF in odontogenic progenitors, dental pulp progenitors were isolated from human un-erupted third molars and the expression of SCF/c-kit in DP cells was examined. Immunofluorescence staining demonstrated that DP cells expressed both SCF (Fig. 1G) and c-Kit (Fig. 1H) proteins. The expression level of SCF protein in DP cells was 1.6 times higher than in PDL, 1.3 higher than in AB, and 1.1 times higher than in DF progenitors (Fig. 1J). Interestingly, c-kit expression was at similar levels in DP, PDL and DF cells, and significantly lower in AB cells (Fig. 1J).

### **Dental pulp progenitors possess dentinogenic/osteogenic potential**

To determine the differentiation potential of DP cells into odontoblast/osteoblast, DP cells were cultured with osteogenic induction medium for 7 and 21 days. Osteogenic conditions resulted in a morphological change of DP cells from an elongated spindle shape to a polygonal shape (Fig. 2A,B). Differentiated DP cells featured higher alkaline phosphatase activity (Fig. 2D versus 2C) and alizarin red staining indicative of mineralization (Fig. 2F versus 2E). In addition, odontoblast-related genes such as DSPP and Nestin were enhanced after treatment with osteogenic induction medium, demonstrating that DP cell can be induced toward an osteoblast/odontoblast lineage using osteogenic medium (Fig. 2G).

### **SCF stimulated proliferation, promoted migration, and enhanced cytoskeletal re-organization of DP progenitors**

To test the effect of SCF on cell proliferation, dental pulp cells were subjected to SCF at a 100nM concentration over a period of 7 days, and cell number was determined in daily intervals during the entire period using an MTT assay. Our data indicated that dental pulp cell number gradually increased in the SCF treated group until a 1.7-fold elevation over the control at day 7 (Fig. 3A). Using a transwell culture system, dental pulp cell number in transwell plates was determined after 24 hours culture and addition of recombinant SCF (Figs. 3B-D). A 20nM SCF concentration increased the number of cultured pulp cells to

144±52.3%, while a 150 nM SCF concentration caused an increase to 265.2±66.4% (Fig. 3E), suggesting that SCF increased the number of migratory dental pulp progenitors. In addition, application of SCF resulted in cytoskeletal rearrangement and actin polymerization of hDPs as visualized by rhodamine-phalloidin staining (Fig. 3G versus Fig. 3F). A G-actin/F-actin ratio *in vivo* assay was used to determine whether SCF affects actin reorganization in DP cells after treatment with SCF (Fig. 3H and I). In this assay, the soluble monomeric G-actin was detected in the supernatant fraction and the polymeric filamentous F-actin was localized in the pellet fraction of whole cell extract. In control DP cells, 58% of the total actin fraction was G-actin and 42% was F-actin. SCF treatment resulted in a reorganization of the actin cytoskeleton by increasing the amount of the polymeric and filamentous F-actin from 42% to 62% (Figs. 3H and I).

### SCF modulated DP cell functions through MEK/ERK and PI3K pathways

To explain the stimulatory effect of SCF on dental pulp cells, we hypothesized that SCF might affect the phosphorylated state of extracellular matrix pathway intermediaries. Our western blot assays confirmed that SCF induced phosphorylation of both AKT and ERK1/2 (Figs. 4A,B). The effect of SCF on ERK phosphorylation was strongest at a concentration of 150nM when tested in a 0-200nM concentration gradient to assess dose dependency (Fig. 4A). Moreover, the elevation of phospho-ERK as a result of SCF application occurred already after one minute, reached a peak after 5 minutes, and decreased thereafter (10 minutes and 30 minutes)(Fig. 4B). To test the involvement of extracellular matrix pathways in SCF induction, PI3K and MEK/ERK pathways were blocked by LY294002 and UO126 pathway inhibitors in the presence of SCF. RhoA expression decreased 2.4-fold after LY294002 treatment and 2-fold after UO126 treatment compared to the SCF treated group, illustrating that SCF affected cell migration through both the PI3K/Akt and MEK/ERK pathways (Fig. 4C,D). In contrast, SCF treatment alone in the absence of PI3K and MEK/ERK pathway inhibitors resulted in a 1.8-fold increase in RhoA, a 12.5-fold increase in phospho-ERK, and a 1.8-fold increase in phospho-AKT expression (Figs. 4C,D). In addition, there was a reduction in the number of migrated cells as a result of LY294002 block to a level of 80.2±27% and a reduction to 69.3±14.2% following UO126 block, while SCF treatment alone caused an increase to 196.2±67.3% (Fig. 4E). To examine whether SCF affected specific cell cycle-related gene expression through the MEK/ERK pathway, SCF effects on FGF2, cyclin D3, and CDK4 gene expression were determined using real-time RT-PCR (Figs. 4F-H). Our analysis revealed a 2-fold increase in FGF2 and cyclin D3 expression and a 7-fold increase in CDK4 expression as a result of SCF treatment after 24 hours of cell culture (Figs. 4F-H). The effect of SCF on cyclin D3 and CDK4 was reduced significantly after application of the ERK inhibitor UO126 (Figs. 4G,H), while UO126 did not affect FGF2 levels after SCF treatment (Fig. 4F). SCF had little effect on FGF2, cyclin D3, and CDK4 gene expression after 48 hours culture (Figs. 4F-H).

### SCF promoted cell homing, angiogenesis as well collagen remodeling and neo-synthesis in subcutaneous implants

To examine the *in vivo* applicability of SCF as a homing factor for stem cell recruitment into implanted tissue scaffolds, subcutaneous collagen sponge implants were treated either with SCF or seeded with dental pulp progenitors or both and harvested after 4 weeks. There was a

7.3-fold increase in cell number in SCF-treated implants when compared to untreated controls (Figs. 5B,E). Dental pulp progenitor (DP) pre-seeding increased cell number 3.2-fold (Figs. 5C,E) and a combination of DP pre-seeding and SCF treatment resulted in an 6.8-fold increase in cell number (Figs. 5D,E). SCF treatment and DP pre-seeding also affected the number of capillaries; SCF treatment alone resulted in a 9.2-fold increase, DP pre-seeding alone in a 2.5-fold increase, and a combination of SCF and DP pre-seeding in an 11-fold increase (Figs. 5A-D, F). The effect of SCF on implant cell number and angiogenesis was highly significant ( $p < 0.0001$ , Figs. 5E,F). In a second study, the effect of SCF on collagen synthesis and remodeling of the subcutaneously implanted collagen scaffold after one week of implantation was assessed (Figs. 5G-M). There was a noticeable degradation of the thick collagen of the implanted scaffold in the SCF treated groups (Figs. 5H and J), and thick scaffold fibers were replaced with thin collagen fibers identified by methyl blue staining (Figs. 5H,J versus G,I). This finding of new collagen fiber formation as a result of SCF treatment was supported by a significant increase in collagen I and III gene expression in SCF-treated groups (Figs. 5K,L). There was also a significant increase in MMP2, an enzyme that degrades denatured collagen I, after SCF treatment (Fig. 5M). Pulp/dentin complex regenerates demonstrated substantial amounts of pre-dentin formation along demineralized dentin surfaces in those groups that contained either dental pulp stem cells or SCF or both (Fig. 5O-Q). The dental pulp stem cell groups also were rich in capillaries/ blood vessels and revealed odontoblast shaped cells perpendicular to the dentin surface ((P,Q).

## Discussion

In the present study we have identified distinct SCF/c-Kit expression patterns in developing mouse molar tooth organs indicating high levels of both SCF and its receptor c-Kit in differentiating dental pulp cells of the sub-odontoblastic region. *In vitro* studies using human dental pulp progenitors demonstrated that SCF up-regulated cell proliferation and migration, and that both the MEK/ERK and the PI3K pathways were involved in modulating the effect of SCF on cell behavior. When applied as an agent to promote tissue regeneration in subcutaneously implanted collagen sponges, SCF promoted cell homing into the implant, angiogenesis, collagen sponge remodeling, and collagen neogenesis. Together, these studies indicate that SCF has powerful effects related to cell homing, angiogenesis, and remodeling, and may be used as a potent aid in mesenchymal tissue regeneration.

The present study for the first time reports the expression of SCF and c-Kit in dental tissues, especially in the dentin/pulp complex. Notably, SCF was highly expressed in odontoblasts and in the subodontoblast cell layer of Höhl [34-36], while c-Kit was detected at higher levels in the pulp and in the subodontoblastic cell layer, when compared to overlying odontoblasts. The overlapping expression of SCF and c-Kit in Höhl cells suggests that during dental pulp development, dimerization of c-Kit with its ligand SCF occurs preferentially in Höhl's preodontoblastic progenitor cell layer, a layer that responds to local injury stimuli and bioactive molecules by proliferation and is considered a source of odontoblast replacement cells [37].



Our study demonstrated co-expression of SCF and c-Kit not only in DP cells, but also in several other types of dental progenitors including dental follicle and periodontal ligament progenitors, suggesting that the SCF/c-Kit system affects other types of odontogenic progenitor populations as well. In DP cells, SCF stimulated cell proliferation in a dose-dependent manner and upregulated cyclin D3 and CDK4 gene expression. These results suggest that SCF acts as a potent mitogen related to DP cells. Expression of c-Kit in dental progenitor cells is likely an important prerequisite for the proliferation and differentiation potential of these cells since the SCF/c-Kit system is known to promote proliferation of mesenchymal progenitors [38-40].

We detected remarkably rapid elevation of ERK1/2 and AKT phosphorylation within minutes following SCF/c-Kit activation in dental pulp cells. Rapid phosphorylation and the role of SCF/c-Kit in the extracellular matrix [30,31] suggests possible involvement of MEK/ERK and PI3K in signaling pathways in modulating the effect of the receptor-ligand interaction on dental pulp progenitors. Blocking ERK1/2 and AKT using inhibitors reduced SCF stimulated dental pulp cell migration and proliferation, confirming that MEK/ERK and PI3K pathways are involved in the SCF-dependent migration and proliferation of dental pulp progenitors. MEK/ERK and PI3K pathways are key pathways in the regulation of key cellular processes such as apoptosis, cell cycle progression, transcription and translation [41]. Previous studies have shown that c-Kit gene silencing or SCF-withdrawal substantially affected ERK and AKT downstream targets and resulted in cell apoptosis [42,43]. In contrast, activation of SCF/c-Kit in dental pulp progenitors may enhance ERK and/or AKT and stimulate dental pulp proliferation and migration, which in turn would be beneficial for dentin/pulp complex tissue engineering through homing strategies.

A role of SCF/c-Kit system in the induction of dental pulp progenitor homing is supported by our finding of enhanced cell migration and cytoskeleton re-arrangement as a result of SCF administration. Our results are supported by a previous study in which c-Kit has been shown to mediate cell attachment to fibronectin, membrane ruffling and filamentous actin assembly in bone marrow derived mast cells [44]. The dramatic effect of the SCF/c-Kit system on DP cell migration through the Rho GTPase pathway and associated cytoskeletal rearrangement might be an important contribution to the physiological response of the dentin/pulp complex to injury. This response involves pulp progenitor migration, proliferation and differentiation at the site of injury, and results in the new generation of odontoblast-like cells, as well as subsequent dentin secretion, a process called reparative dentinogenesis [35]. Thus, as an agent for the dental pulp/dentin complex homing, SCF-mediated progenitor homing exploits the dental pulp's natural defense mechanism against toxic or mechanical injury for the purpose of new pulp tissue and dentin formation.

The present study indicates that application of SCF in dental pulp regeneration not only induced chemotaxis but also promoted angiogenesis, remodeling of implanted collagen scaffolds, and new collagen matrix synthesis. Specifically, SCF resulted in 10-fold increase in the number of capillaries, a significant increase in collagens I and III levels, as well as elevated levels of MMP2, the latter likely responsible for the degradation of the collagen implant scaffold. The effect of SCF on neovascularization has been reported in previous studies and might be explained by its activation of endothelial progenitors [45,46].

Moreover, endothelial-specific markers have been detected in human dental pulp stem cells, demonstrating their angiogenic potential [47]. Our studies implicate that SCF may induce DP cell differentiation toward an angiogenic lineage. Little is known about the effect of SCF on metalloproteinases, while the effect of the SDF-1 chemokine on MMP-2, MMP-8, and MMP-9 secretion and activity is well established [48,49]. Such metalloproteinase activity is therapeutically beneficial for the degradation of engrafted collagen constructs in tissue engineering. Addition of SCF appeared to also stimulate the formation of a finely structured network of new collagen fibers in our study, a finding that was supported by the upregulation of collagen I and III. The effect of SCF on collagen expression has not yet been described, but previous reports have shown an involvement of the CXCR4-SDF1 axis in collagen invasion [50].

Together, our implantation studies establish that in addition to the induction of migration, proliferation, and chemotaxis, SCF also promotes an array of other benefits related to tissue engineering, including neovascularization, degradation of exogenous collagen scaffolds, and new collagen fiber formation. These benefits may propel chemokines such as SDF-1 and SCF toward the forefront of homing factors for tissue engineering. However, a word of caution may be appropriate because of the effect of SCF on MEK/ERK and PI3K/AKT pathways, as demonstrated in the present study. These pathways have been linked to tumorigenesis [51], and also SDF-1 has been associated with angiogenesis and tumor growth [52]. Our tissue engineered constructs have not shown any tumorigenesis so far, but further studies may be needed to ensure the long-term clinical safety of these highly potent chemokines.

## Acknowledgment

Generous funding by NIDCR grant DE019463 to XL is gratefully acknowledged.

## References

1. Frenette PS, Subbarao S, Mazo IB, von Andrian UH, Wagner DD. Endothelial selectins and vascular cell adhesion molecule-1 promote hematopoietic progenitor homing to bone marrow. *Proc Natl Acad Sci U S A*. 1998; 95(24):14423–8. [PubMed: 9826716]
2. Cheng Z, Ou L, Zhou X, et al. Targeted migration of mesenchymal stem cells modified with CXCR4 gene to infarcted myocardium improves cardiac performance. *Mol Ther*. 2008; 16(3):571–9. [PubMed: 18253156]
3. Yagi H, Soto-Gutierrez A, Parekkadan B, et al. Mesenchymal stem cells: Mechanisms of immunomodulation and homing. *Cell Transplant*. 2010; 19(6):667–79. [PubMed: 20525442]
4. Chen FM, Wu LA, Zhang M, Zhang R, Sun HH. Homing of endogenous stem/progenitor cells for in situ tissue regeneration: Promises, strategies, and translational perspectives. *Biomaterials*. 2011; 32(12):3189–209. [PubMed: 21300401]
5. Lapidot T, Dar A, Kollet O. How do stem cells find their way home? *Blood*. 2005; 106(6):1901–10. [PubMed: 15890683]
6. Fong EL, Chan CK, Goodman SB. Stem cell homing in musculoskeletal injury. *Biomaterials*. 2011; 32(2):395–409. [PubMed: 20933277]
7. Min JY, Huang X, Xiang M, et al. Homing of intravenously infused embryonic stem cell-derived cells to injured hearts after myocardial infarction. *J Thorac Cardiovasc Surg*. 2006; 131(4):889–97. [PubMed: 16580449]
8. Kim JY, Xin X, Moioli EK, et al. Regeneration of dental-pulp-like tissue by chemotaxis-induced cell homing. *Tissue Eng Part A*. 2010; 16(10):3023–31. [PubMed: 20486799]

9. Kim K, Lee CH, Kim BK, Mao JJ. Anatomically shaped tooth and periodontal regeneration by cell homing. *J Dent Res*. 2010; 89(8):842–7. [PubMed: 20448245]
10. Suzuki T, Lee H, Chen M, et al. Induced migration of dental pulp stem cells for in vivo pulp regeneration. *J dent Res*. 2011; 90(8):1013–8. [PubMed: 21586666]
11. Huang GT, Yamaza T, Shea LD, et al. Stem/progenitor cell-mediated de novo regeneration of dental pulp with newly deposited continuous layer of dentin in an in vivo model. *Tissue Eng Part A*. 2010; 16(2):605–15. [PubMed: 19737072]
12. Dangaria SJ, Ito Y, Luan X, Diekwisch TG. Successful periodontal ligament regeneration by periodontal progenitor preseeding on natural tooth root surfaces. *Stem Cells Dev*. 2011; 20(10):1659–68. [PubMed: 21250830]
13. Dangaria SJ, Ito Y, Yin L, Valdre G, Luan X, Diekwisch TG. Apatite microtopographies instruct signaling tapestries for progenitor-driven new attachment of teeth. *Tissue Eng Part A*. 2011; 17(3-4):279–90. [PubMed: 20795795]
14. Cordeiro MM, Dong Z, Kaneko T, et al. Dental pulp tissue engineering with stem cells from exfoliated deciduous teeth. *J Endod*. 2008; 34(8):962–9. [PubMed: 18634928]
15. Casagrande L, Cordeiro MM, Nor SA, Nor JE. Dental pulp stem cells in regenerative dentistry. *Odontology*. 2011; 99(1):1–7. [PubMed: 21271319]
16. Sakai VT, Cordeiro MM, Dong Z, Zhang Z, Zeitlin BD, Nor JE. Tooth slice/scaffold model of dental pulp tissue engineering. *Adv Dent Res*. 2011; 23(3):325–32. [PubMed: 21677087]
17. Yan M, Yu Y, Zhang G, Tang C, Yu J. A journey from dental pulp stem cells to a bio-tooth. *Stem Cell Rev*. 2011; 7(1):161–71. [PubMed: 20506048]
18. Iohara K, Imabayashi K, Ishizaka R, et al. Complete pulp regeneration after pulpectomy by transplantation of CD105+ stem cells with stromal cell-derived factor-1. *Tissue Eng Part A*. 2011; 17(15-16):1911–20. [PubMed: 21417716]
19. Kollet O, Shvitiel S, Chen YQ, et al. HGF, SDF-1, and MMP-9 are involved in stress-induced human CD34+ stem cell recruitment to the liver. *J Clin Invest*. 2003; 112(2):160–9. [PubMed: 12865405]
20. Swenson ES, Kuwahara R, Krause DS, Theise ND. Physiological variations of stem cell factor and stromal-derived factor-1 in murine models of liver injury and regeneration. *Liver Int*. 2008; 28(3):308–18. [PubMed: 18290773]
21. Dutt P, Wang JF, Groopman JE. Stromal cell-derived factor-1 alpha and stem cell factor/kit ligand share signaling pathways in hemopoietic progenitors: a potential mechanism for cooperative induction of chemotaxis. *J Immunol*. 1998; 161(7):3652–8. [PubMed: 9759889]
22. Lennartsson J, Blume-Jensen P, Hermanson M, Ponten E, Carlberg M, Ronnstrand L. Phosphorylation of Shc by Src family kinases is necessary for stem cell factor receptor/c-kit mediated activation of the Ras/MAP kinase pathway and c-fos induction. *Oncogene*. 1999; 18(40):5546–53. [PubMed: 10523831]
23. Edling CE, Hallberg B. c-Kit--a hematopoietic cell essential receptor tyrosine kinase. *Int J Biochem Cell Biol*. 2007; 39(11):1995–8. [PubMed: 17350321]
24. McNiece IK, Briddell RA. Stem cell factor. *J Leukoc Biol*. 1995; 58(1):14–22. [PubMed: 7542304]
25. Smith MA, Court EL, Smith JG. Stem cell factor: laboratory and clinical aspects. *Blood Rev*. 2001; 15(4):191–7. [PubMed: 11792120]
26. Yaniz-Galende E, Chen J, Chemaly ER, et al. Stem cell factor gene transfer promotes cardiac repair after myocardial infarction via in situ recruitment and expansion of c-kit+ cells. *Circ Res online*. 2012
27. Jin K, Mao XO, Sun Y, Xie L, Greenberg DA. Stem cell factor stimulates neurogenesis in vitro and in vivo. *J Clin Invest*. 2002; 110(3):311–9. [PubMed: 12163450]
28. Miyamoto K, Kobayashi T, Hayashi Y, et al. Involvement of stem cell factor and c-kit in corneal wound healing in mice. *Mol Vis*. 2012; 18:1505–15. [PubMed: 22736941]
29. Sette C, Dolci S, Geremia R, Rossi P. The role of stem cell factor and of alternative c-kit gene products in the establishment, maintenance and function of germ cells. *Int J Dev Biol*. 2000; 44(6):599–608. [PubMed: 11061423]
30. Broudy VC. Stem cell factor and hematopoiesis. *Blood*. 1997; 90(4):1345–64. [PubMed: 9269751]

31. Reber L, Da Silva CA, Frossard N. Stem cell factor and its receptor c-Kit as targets for inflammatory diseases. *Eur J Pharmacol.* 2006; 533(1-3):327–40. [PubMed: 16483568]
32. Dangaria S, Ito Y, Luan X, Diekwisch GHT. Differentiation of neural-crest-derived intermediate pluripotent progenitors into committed periodontal population involved unique molecular signature changes, cohort shifts and epigenetic modifications. *Stem Cells Dev.* 2011; 20(1):39–52. [PubMed: 20604680]
33. Livak KJ, Schmittgen TD. Analysis of relative gene expression data using real-time quantitative PCR and the 2<sup>-</sup>(Delta Delta C(T)) Method. *Methods.* 2001; 25(4):402–8. [PubMed: 11846609]
34. Tziafas D. Basic mechanisms of cytodifferentiation and dentinogenesis during dental pulp repair. *Int J Dev Biol.* 1995; 39(1):281–90. [PubMed: 7626418]
35. Tziafas D, Smith AJ, Lesot H. Designing new treatment strategies in vital pulp therapy. *J Dent.* 2000; 28(2):77–92. [PubMed: 10666965]
36. Goldberg M, Smith AJ. Cells and Extracellular Matrices of Dentin and Pulp: A Biological Basis for Repair and Tissue Engineering. *Crit Rev Oral Biol Med.* 2004; 15(1):13–27. [PubMed: 14761897]
37. Sloan AJ, Shelton RM, Hann AC, Moxham BJ, Smith AJ. An in vitro approach for the study of dentinogenesis by organ culture of the dentine-pulp complex from rat incisor teeth. *Arch Oral Biol.* 1998; 43(6):421–30. [PubMed: 9717580]
38. Sun S, Guo Z, Xiao X, et al. Isolation of mouse marrow mesenchymal progenitors by a novel and reliable method. *Stem Cells.* 2003; 21(5):527–35. [PubMed: 12968107]
39. Huss R, Moosmann S. The co-expression of CD117 (c-kit) and osteocalcin in activated bone marrow stem cells in different diseases. *Br J Haematol.* 2002; 118(1):305–12. [PubMed: 12100166]
40. Hall FL, Han B, Kundu RK, Yee A, Nimni ME, Gordon EM. Phenotypic differentiation of TGF-beta1-responsive pluripotent premesenchymal prehematopoietic progenitor (P4 stem) cells from murine bone marrow. *J Hematother Stem Cell Res.* 2001; 10(2):261–71. [PubMed: 11359673]
41. Chappell WH, Steelman LS, Long JM, et al. Ras/Raf/MEK/ERK and PI3K/PTEN/Akt/mTOR inhibitors: rationale and importance to inhibiting these pathways in human health. *Oncotarget.* 2011; 2(3):135–64. [PubMed: 21411864]
42. Li H, Wang X, Li N, Qiu J, Zhang Y, Cao X. hPEBP4 resists TRAIL-induced apoptosis of human prostate cancer cells by activating Akt and deactivating ERK1/2 pathways. *J Biol Chem.* 2007; 282(7):4943–50. [PubMed: 17178731]
43. Lim SC, Duong HQ, Choi JE, Parajuli KR, Kang HS, Han SI. Implication of PI3K-dependent HSP27 and p53 expression in mild heat shock-triggered switch of metabolic stress-induced necrosis to apoptosis in A549 cells. *Int J Oncol.* 2010; 36(2):387–93. [PubMed: 20043073]
44. Vosseller K, Stella G, Yee NS, Besmer P. c-kit receptor signaling through its phosphatidylinositide-3'-kinase-binding site and protein kinase C: role in mast cell enhancement of degranulation, adhesion, and membrane ruffling. *Mol Biol Cell.* 1997; 8(5):909–22. [PubMed: 9168474]
45. Kim KL, Meng Y, Kim JY, Baek EJ, Suh W. Direct and differential effects of stem cell factor on the neovascularization activity of endothelial progenitor cells. *Cardiovasc Res.* 2011; 92(1):132–40. [PubMed: 21636540]
46. Elmasri H, Ghelfi E, Yu CW, et al. Endothelial cell-fatty acid binding protein 4 promotes angiogenesis: role of stem cell factor/c-kit pathway. *Angiogenesis.* 2012; 15(3):457–68. [PubMed: 22562362]
47. Marchionni C, Bonsi L, Alviano F, et al. Angiogenic potential of human dental pulp stromal (stem) cells. *Int J Immunopathol Pharmacol.* 2009; 22(3):699–706. [PubMed: 19822086]
48. Janowska-Wieczorek A, Marquez LA, Dobrowsky A, Ratajczak MZ, Cabuhat ML. Differential MMP and TIMP production by human marrow and peripheral blood CD34(+) cells in response to chemokines. *Exp Hematol.* 2000; 28(11):1274–85. [PubMed: 11063876]
49. Shen X, Wang S, Wang H, Liang M, Xiao L, Wang Z. The role of SDF-1/CXCR4 axis in ovarian cancer metastasis. *J Huazhong Univ Sci Technol Med Sci.* 2009; 29(3):363–7. [PubMed: 19513623]

50. Barbolina MV, Kim M, Liu Y, et al. Microenvironmental regulation of chemokine (C-X-C-motif) receptor 4 in ovarian carcinoma. *Mol Cancer Res.* 2010; 8(5):653–64. [PubMed: 20460402]
51. McCubrey JA, Steelman LS, Abrams SL, et al. Roles of the RAF/MEK/ERK and PI3K/PTEN/AKT pathways in malignant transformation and drug resistance. *Adv Enzyme Regul.* 2006; 46(2):249–79. [PubMed: 16854453]
52. Orimo A, Gupta PB, SgROI DC, et al. Stromal fibroblasts present in invasive human breast carcinomas promote tumor growth and angiogenesis through elevated SDF-1/CXCL12 secretion. *Cell.* 2005; 121(3):335–48. [PubMed: 15882617]

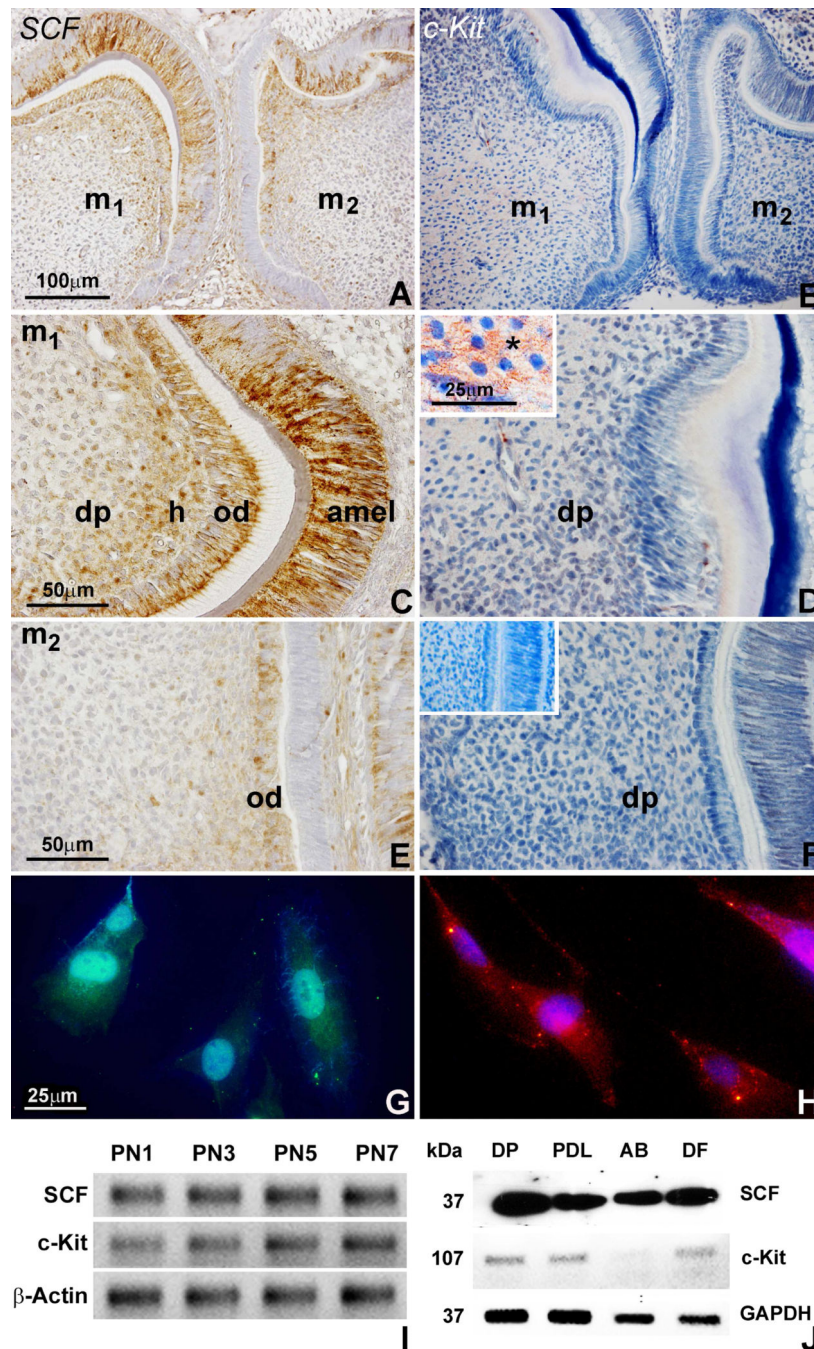


**Figure 1. SCF/c-Kit expression and localization during mouse dentinogenesis and in dental pulp progenitors**

(A-F) Immunostained sections of first and second molars from 3 day postnatal mice demonstrating SCF and c-Kit protein localization in the dental pulp (dp), odontoblasts (ob), and ameloblasts (amel). The SCF protein was highly expressed and specifically localized in odontoblasts, Höhl's subodontoblastic layer (h), and adjacent dental pulp of first and second molars (A,C,E). SCF was also detected in secretory ameloblasts (amel)(C). In contrast, the c-Kit protein was evenly distributed in the first molar dental pulp (B,D), and only detected at low levels in the pulp of the second molar (F). The insert (D) illustrates the c-Kit protein

network on the surface of dental pulp cells. The second insert (F) is a matching micrograph of an immunostaining control reaction. (G,H) Immunofluorescent analysis of SCF (G) and c-Kit (H) protein localization in dental pulp progenitors. (I) RT-PCR analysis of SCF and c-Kit mRNA expression in the dental papilla from 1, 3, 5, and 7 days postnatal mice. The  $\beta$ -Actin gene was used as internal control. (J) Western blot analysis of SCF and c-Kit protein expression in the dental pulp (DP), periodontal ligament (PDL), alveolar osteoblast (AB) and dental follicle (DF) progenitors. Cell extracts were processed for immunoblotting with antibodies against SCF and c-Kit. GAPDH was detected as a loading control. Note that SCF protein expression was highest in dental pulp and lowest in alveolar osteoblast cells.

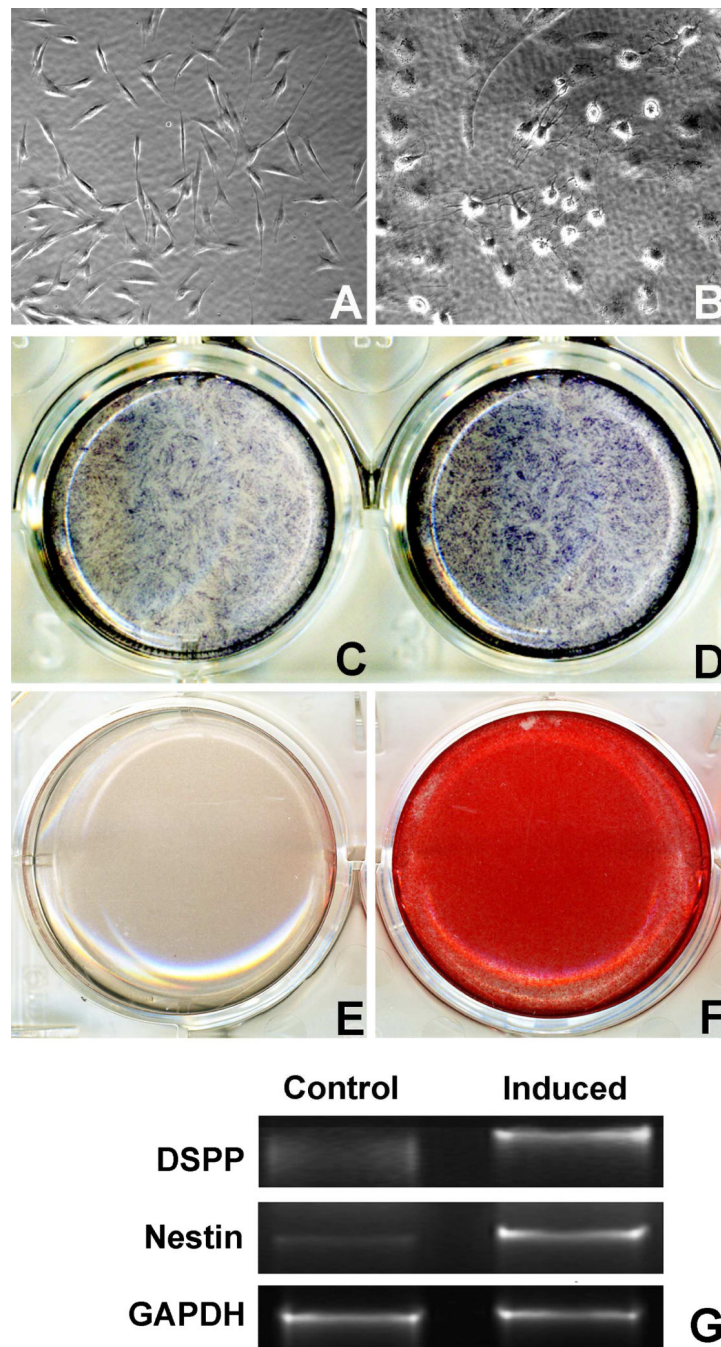


**Figure 2. Osteogenic potential of dental pulp progenitors**

(A,B) Phase contrast images of DP cells before and after osteogenic induction. Note that DP cell shape changed during osteogenic differentiation. (C,D) Alkaline phosphatase activity staining at day 7 of culture identified differentiated cells positive for alkaline phosphatase with blue staining. (E,F) Alizarin red staining for mineral nodule formation. Cells were cultured for 21 days with or without osteogenic induction. Mineral nodules were stained in red. All experiments were carried out in triplicate and repeated three times. (G) RT-PCR



analysis of DSPP and Nectin gene expression in un-differentiated or differentiated DP cells. The GAPDH gene was used as an internal control.

Author Manuscript

Author Manuscript

Author Manuscript

Author Manuscript

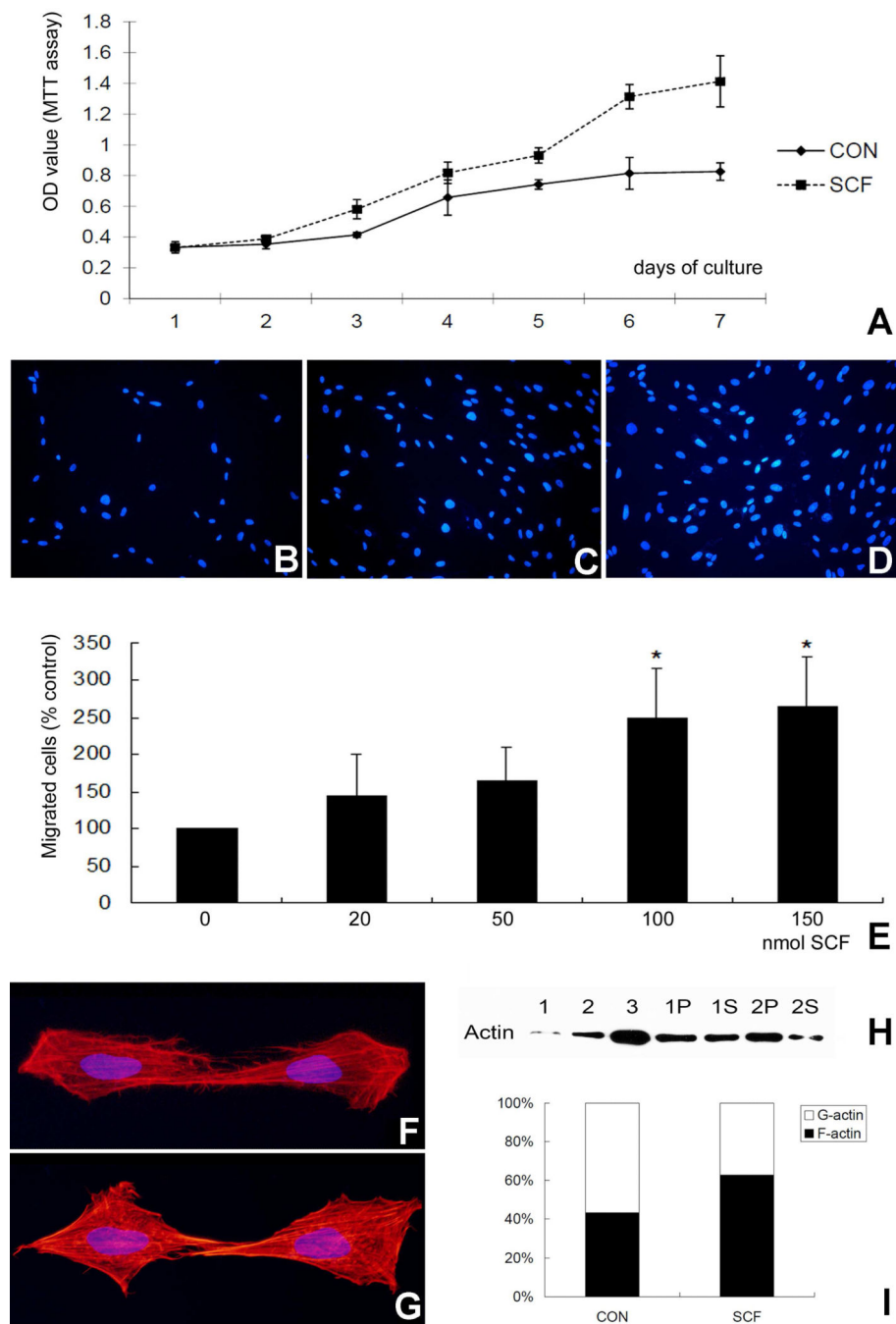


**Figure 3. Effect of SCF on DP cell proliferation, migration, and cytoskeletal reorganization** (A) Comparison between SCF treated (100nM) and control DP cell proliferation over a 7 day culture period using the MTT assay. The measured absorbance (mean $\pm$ SD) is proportionate to the number of living cells. (B-D) DAPI staining of migrated DP cell nuclei on fluorescence blocking PET membranes. For this assay, DP cells were seeded into culture inserts and 50 nM BSA (B), 50nM SCF (C), or 150nM SCF (D) were added to lower wells. After 24 hours culture, fluorescent micrographs were taken of cells on the DAPI stained membranes. (E) Dose-dependent effect of SCF on the number of migrated and DAPI stained

DP cells. The number of migrated cells on each membrane was counted and graphed using the BSA-treated group as 100%. (F,G) Fluorescent images of rhodamine-phalloidin-stained F-actin. The number of stress fibers increased as a result of SCF treatment (G). (H) Western blot analysis of actin reorganization in DP cells after treatment with SCF as demonstrated using a G-actin/F-actin ratio *in vivo* assay. The soluble monomeric G-actin was detected in the supernatant fraction and the polymeric filamentous F-actin was localized in the pellet fraction of whole cell extract. 1-3 are actin protein controls, 1P and 1S are the control pellet (P) and supernatant (S), while 2P and 2S are pellet and supernatant after SCF treatment. SCF treatment resulted in an accumulation of F-actin in the pellet fraction. (I) Changes in the G-actin and F-actin ratio in DP cells treated with SCF. G-actin is the white portion and F-actin is the black colored portion of the bar graph. Note the increase percentage of F-actin as a result of SCF treatment. \*  $p < 0.05$ .

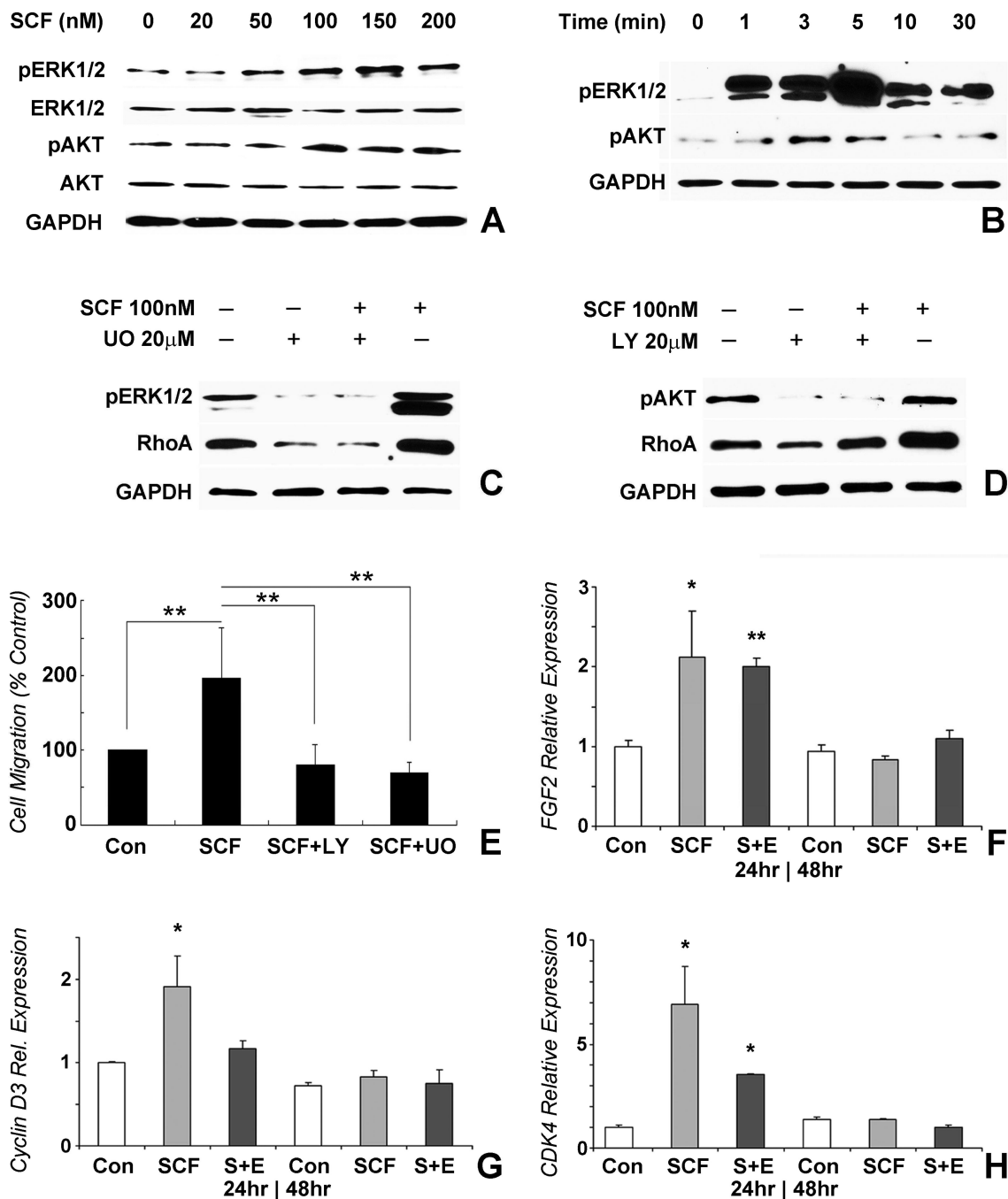


**Figure 4. SCF modulated DP cell function through ERK and PI3K pathways**

DP cells were seeded into 6-well plates at  $5 \times 10^5$ /well and cultured for pre-determined time intervals. SCF alone or SCF plus ERK/AKT inhibitor were then added to culture medium. (A) Western blot analysis of the dose-dependent effect of SCF on the phosphorylated state of ERK and AKT in DP cells. (B) Time course of the SCF effect on the phosphorylated state of ERK and AKT. (C) Inhibition of the SCF effect on ERK phosphorylation and RhoA protein expression by the ERK inhibitor. (D) Inhibition of the SCF effect on AKT phosphorylation and RhoA expression by the PI3K inhibitor. SCF function was selectively inhibited with the

ERK inhibitor UO126, or the PI3K inhibitor LY 294002. (E) Blockage of the SCF effect on cell migration by both ERK and PI3K inhibitors. (F-H) Real-time RT-PCR analysis of cell proliferation related gene expression in dental pulp progenitors treated with SCF only or SCF (SCF) plus ERK inhibitor (S+E) compared to controls (Con) and after 24 or 48 hours cell culture. Levels of gene expression of FGF2 (F), Cyclin D3 (G), and CDK4 (H) were calculated relative to control group gene expression levels after 24 and 48 hours of culture. \*  $p < 0.05$ , \*\*  $p < 0.01$ .

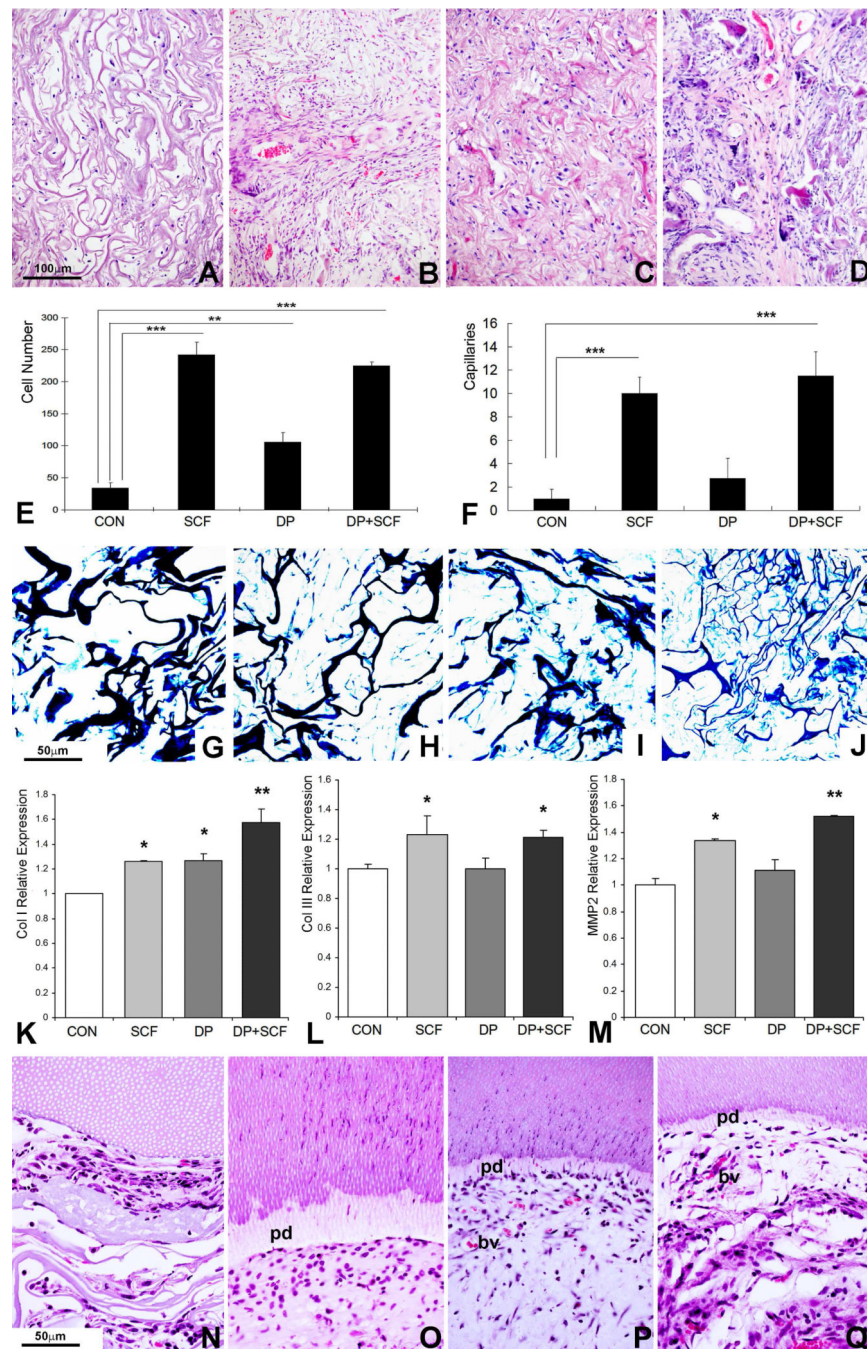


### Figure 5. Effect of SCF on cell homing and dental pulp regeneration in vivo

Collagen sponges were treated either with SCF or seeded with DP cells or both, and subcutaneously implanted into nude mice for 1 or 4 weeks. (A-D) H & E staining of collagen sponge implants subjected to four different types of treatment: collagen sponge control (A), collagen sponge treated with SCF (B), collagen sponge seeded with DP cells (C) and collagen sponge seeded with DP cells and treated with SCF (D). Note the formation of pulp-like tissues in the two groups in which the scaffold was seeded with pulp progenitors (C,D versus A,B). (E) Cell number per field averaging three different implants per group.

Four treatment groups were compared: collagen implant without cells (Con), collagen implant treated with SCF but without cells (SCF), collagen implant with dental pulp progenitors (DP), and collagen implant with dental pulp progenitors and SCF treatment (DP +SCF). (F) Number of capillaries per field averaging three different implants and using the same four treatment groups described in (E). (G-J) Visualization of collagen fibers in subcutaneous implants using methyl blue staining comparing four groups of treatment: collagen sponge control (G), collagen sponge treated with SCF (H), collagen sponge seeded with DP cells (I) and collagen sponge seeded with DP cells and treated with SCF (J). Note the degradation of thick collagen fibers and replacement with thin fibers forming smaller subunits in the SCF treated groups (H,J versus G,I). (K-M) Real-time RT-PCR analysis of matrix remodeling related gene expression in subcutaneous implants subjected to dental pulp progenitor preseeding and SCF treatment (groups as in E,F). Levels of gene expression of Collagen I (K), Collagen III (L), and MMP2 (M) were calculated relative to control group gene expression levels. (N-Q) Micrographs of decalcified and H&E stained sections from co-implanted tooth slice/pulp regenerates. Tooth slice/pulp regenerates were implanted subcutaneously for four weeks. The four groups were collagen sponge alone (N), collagen sponge plus SCF (O), collagen sponge plus dental pulp stem cells (P), and sponge plus SCF plus dental pulp stem cells (Q). Note a new layer of predentin (pd) in the groups treated either with SCF or stem cells or both (O-Q). The two groups treated with dental pulp stem cells featured small capillaries (bv)(P,Q). Only the dental pulp stem cell groups featured odontoblast like cells oriented perpendicular to the dentin surface (P,Q), while the group treated with SCF alone displayed oval-shaped round cells parallel to the dentin surface (O). \*  $p < 0.05$ , \*\*  $p < 0.01$ , \*\*\*  $p < 0.001$ .

**Table 1**

## Primer sequences for RT PCR analysis

Human CDK4	5'CCTGAGGTCAGGAGTTCGAG 3'CCACCACGCCTGACTAATTT
Human Cyclin D3	5'TGCTGACAGCTGCTCCTAGA 3'AGCTGAGCAGAAAGCAAAGC
Human DSPP	5'GAAGATGCTGGCCTGGATAA 3'CATCACCAGAACCCTCGTCT
Human FGF2	5'AAAAATAGCCAGGCATGGTG 3'ACCTTGACCTCTCAGCCTCA
Human Nestin	5'AACAGCGACGGAGGTCTCTA 3'TTCTCTTGCCCGCAGACTT
Human $\beta$ -Actin	5'TTGCTGACAGGATGCAGAAG 3'GTA CT TGCGCTCAGGAGGAG
Mouse c-Kit	5'TCATCGAGTGTGATGGGAAA 3'CACGTTTTTGATGGTGATGC
Mouse Col I	5'ACTGGTACATCAGCCGAAC 3'TACTCGAACGGGAATCCATC
Mouse Col III	5'ACCAAAAAGGTGATGCTGGAC 3'GACCTCGTGCTCCAGTTAGC
Mouse MMP2	5'TGGGGGAGATTCTCACTTTG 3'CCATCAGCGTTCCATACTT
Mouse SCF	5'CCGCTCTCTTTGGATCTCAG 3'GTGTGGCATAAGGGCTCACT
Mouse GAPDH	5'AACTTTGGCATTGTGGAAGG 3'GGATGCAGGGATGATGTTCT